ADVANCES IN ATMOSPHERIC SCIENCES, VOL. 23, NO. 1, 2006, 33–44

Application of an Error Statistics Estimation Method to the PSAS Forecast Error Covariance Model

Runhua YANG[*1,4], Jing GUO[2,4], and Lars Peter RIISHØJGAARD[3,4]

[1]*Science Systems and Applications Inc., Lanham, USA*

[2]*Science Applications International Corporation, Beltsville, USA*

[3]*Joint Center for Earth Systems Technology/UMBC, Baltimore, USA*

[4]*Global Modeling and Assimilation Office, NASA Goddard Space Flight Center, Greenbelt, USA*

(Received 25 February 2005; revised 25 July 2005)

ABSTRACT

In atmospheric data assimilation systems, the forecast error covariance model is an important component. However, the parameters required by a forecast error covariance model are difficult to obtain due to the absence of the truth. This study applies an error statistics estimation method to the Physical-space Statistical Analysis System (PSAS) height-wind forecast error covariance model. This method consists of two components: the first component computes the error statistics by using the National Meteorological Center (NMC) method, which is a lagged-forecast difference approach, within the framework of the PSAS height-wind forecast error covariance model; the second obtains a calibration formula to rescale the error standard deviations provided by the NMC method. The calibration is against the error statistics estimated by using a maximum-likelihood estimation (MLE) with rawindsonde height observed-minus-forecast residuals. A complete set of formulas for estimating the error statistics and for the calibration is applied to a one-month-long dataset generated by a general circulation model of the Global Model and Assimilation Office (GMAO), NASA. There is a clear constant relationship between the error statistics estimates of the NMC-method and MLE. The final product provides a full set of 6-hour error statistics required by the PSAS height-wind forecast error covariance model over the globe. The features of these error statistics are examined and discussed.

Key words: forecast error statistics estimation, data analysis, forecast error covariance model

1. Introduction

In atmospheric data assimilation systems, it is important to represent appropriate height-wind forecast error covariance. This error covariance governs the filtering of the observations and the spatial multivariate interpolation of the filtered observations (Hollingsworth, 1989). However, the error statistics required by a forecast error covariance model is difficult to obtain due to the absence of the truth. A number of different methods are widely used to provide the estimates.

Recently, Ingleby reviewed three ways of estimating forecast errors (Ingleby, 2001) and pointed out the strengths and the weakness of each method. The first method is to compare the forecast with observations, such as the outstanding studies of Hollingsworth and Lönnberg (1986) and Lönnberg and Hollingsworth (1986). In their studies, they found the basic statistical features of height and wind forecast error and a geostrophic-like balance between the errors of height and wind by comparing the forecast with verified radiosonde data over North America. However, the observation method is limited by data sparsity and by the situation when the analysis variables are not the same as the observed.

The second method is the Kalman filter type that provides a temporal evolution of forecast error statistics. However, due to its computational cost and requirements for an estimation of model error, this method has not been used in operational systems yet.

The third method, called the National Meteorological Center (NMC) method (Parrish and Derber, 1992), provides global multivariate correlations valid for the full horizontal and vertical extent of the model domain, and has been adopted by several weather forecast operational centers recently. The basic assumption behind the method is that differences between two forecasts

*E-mail: ryang@gmao.gsfc.nasa.gov

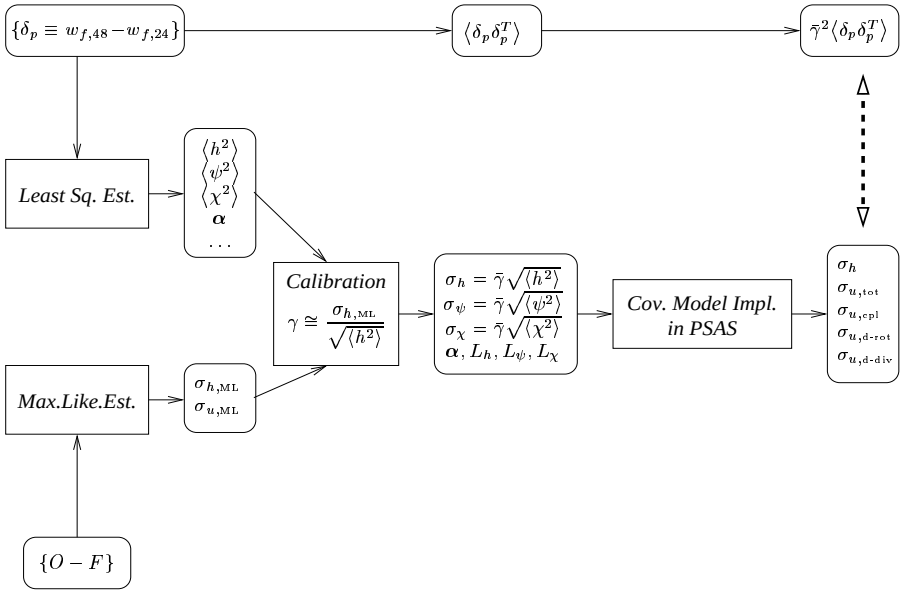

Fig. 1. Schematic of the components and procedures of the method employed in this study. Upper part outlines the computation in the NMC-method, and the bottom part is for MLE. See the text for the meanings of the symbols.

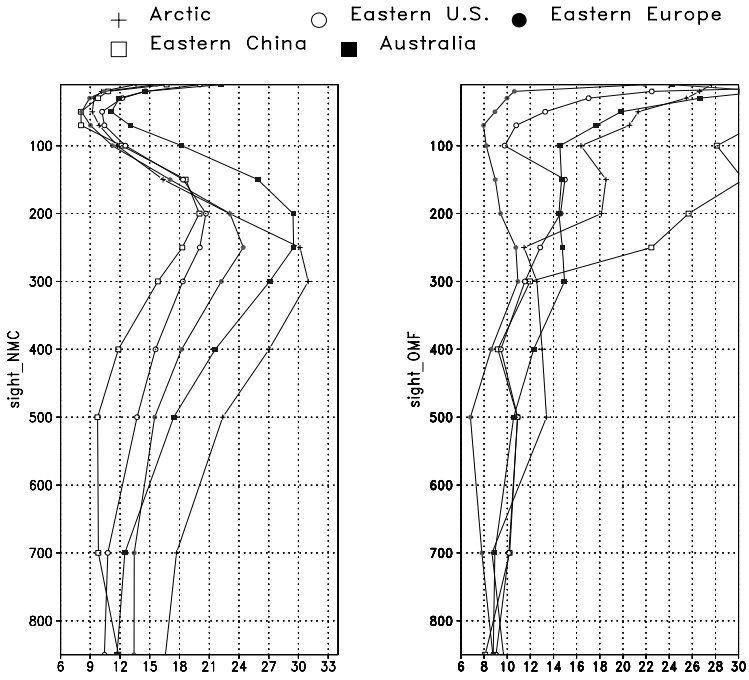

Fig. 2. Left: regional mean standard deviation derived from forecast height difference using the NMC-method (sight_NMC) over the five regions; right: similar to the left panel, but for the results of MLE (sight_OMF).

at different ranges valid at the same time can be used as proxies for actual forecast errors. Such lagged-forecast differences are easy to obtain, and it is easy to generate the various required statistics from them.

In the practice of the NMC-method, two common questions are raised: how to justify the basic assump-

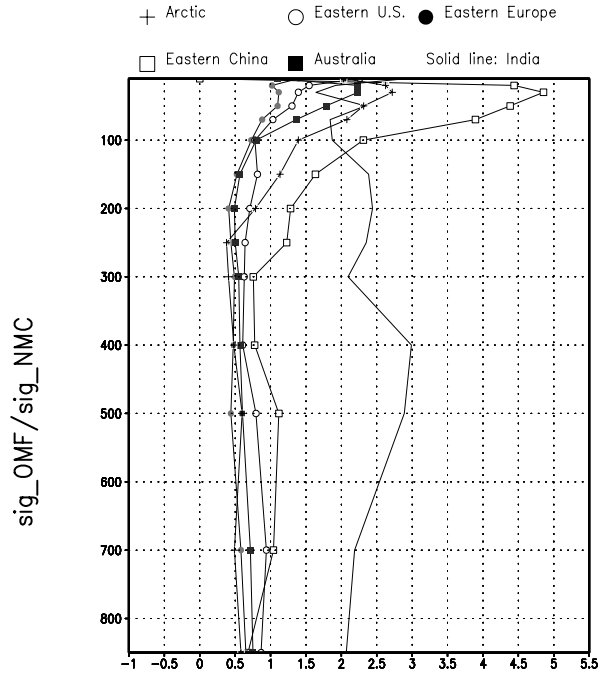

Fig. 3. Ratio of the forecast height standard deviation derived from MLE (sig_OMF) to that derived from the NMC-method (sig_NMC) over the six regions.

tion; and how to rescale the estimated error statistics to represent the 6-hour forecast errors. The latter typically needs to use some form of independent information.

In this study, we employ a method (Guo, 2005) aimed at the second question: to rescale the forecast error statistics of the NMC-method by using independent observation data. The method consists of two components: the first one is to derive error statistics using the NMC-method within the framework of a given height-wind covariance model; the second is to calibrate those statistics against the 6-hour forecast error estimates obtained by a maximum-likelihood estimation (MLE, Dee and Da Silva, 1999) with raw-insonde observed-minus-forecast residuals or innovations. The method is used to estimate the statistics required by the height-wind forecast error covariance model implemented in the Physical-space Statistical Analysis System (PSAS), developed at the Data Assimilation Office (DAO, now the Global Modeling and Assimilation Office, National Aeronautics and Space Administration/Godard Space Flight Center (NASA/GSFC). The final product provides a full set of global error statistics with the pattern dynamically constrained by the model, an NMC-method feature, and with the magnitude of the 6-hour forecast error variance obtained from MLE.

This paper is organized as follows. Section 2 presents the height-wind error relationship prescribed in PSAS and a brief overview of the NMC-method and MLE. Section 3 exhibits the regional means of the forecast error statistics obtained by MLE and the comparison with the results of the NMC-method. It also describes the considerations leading to the choice of a calibration formula, the calibration procedures, and the experiment with these rescaled error statistics as the input of the PSAS error covariance model. In section 4, the components of the wind error variance produced by the PSAS covariance model are examined to verify the consistency between the method and the model. The impact of the error horizontal correlation length on the results is shown also. The final section is devoted to the summary of the main results and the merits of this method.

2. Height-wind error relationship, NMC-method, and MLE

2.1 *Height-wind error relationship in PSAS*

In the PSAS algorithm, a multivariate height-wind error covariance is applied to wind and height analysis. The algorithm can, at least in principle, accommodate a flexible three-dimensional error specification since the analysis equation is solved in observation and physical space. The wind error is given as the sum of two components: one is coupled to the geopotential height error through a basic mass-wind balance relation (geostrophy), while the other is uncoupled from the errors in the mass field (Guo et al., 1998). The mass-coupled wind errors $(u_{\rm c}, v_{\rm c})$ are modeled in terms of the height error h by assuming the following linear relationship:

$$\begin{pmatrix} u_{\rm c} \\ v_{\rm c} \end{pmatrix} \equiv \frac{g}{2\Omega a} \begin{pmatrix} \alpha_{u{\rm m}} & \alpha_{u{\rm l}} \\ \alpha_{v{\rm m}} & \alpha_{v{\rm l}} \end{pmatrix} \begin{pmatrix} h_{\rm m} \\ h_{\rm l} \end{pmatrix}. \quad (1)$$

The height-decoupled wind errors $(u_{\rm d}, v_{\rm d})$ are specified as:

$$\begin{pmatrix} u_{\rm d} \\ v_{\rm d} \end{pmatrix} \equiv \frac{g}{2\Omega a} \begin{pmatrix} -\psi_{\rm m} + \chi_{\rm l} \\ \psi_{\rm l} + \chi_{\rm m} \end{pmatrix}. \quad (2)$$

Here, $\alpha_{u{\rm m}}, \alpha_{u{\rm l}}, \alpha_{v{\rm m}}$ and $\alpha_{v{\rm l}}$ are coefficients coupling the height error gradient in the latitudinal (meridional, m) or longitudinal (l) direction to the error in the u and v components, respectively. The acceleration due to gravity is denoted by g, Ω is the angular velocity of the Earth rotation, and a is the radius of the Earth. The streamfunction and velocity-potential of the height-decoupled wind errors are denoted by ψ and χ, respectively, and $h_{\rm m} \equiv \partial_{\rm m} h; h_{\rm l} \equiv \partial_{\rm l} h; \psi_{\rm m} \equiv \partial_{\rm m}\psi; \psi_{\rm l} \equiv \partial_{\rm l}\psi; \chi_{\rm m} \equiv \partial_{\rm m}\chi$; and $\chi_{\rm l} \equiv \partial_{\rm l}\chi$. Symbols $\partial_{\rm m}$ and $\partial_{\rm l}$ denote differentiation operators, defined as

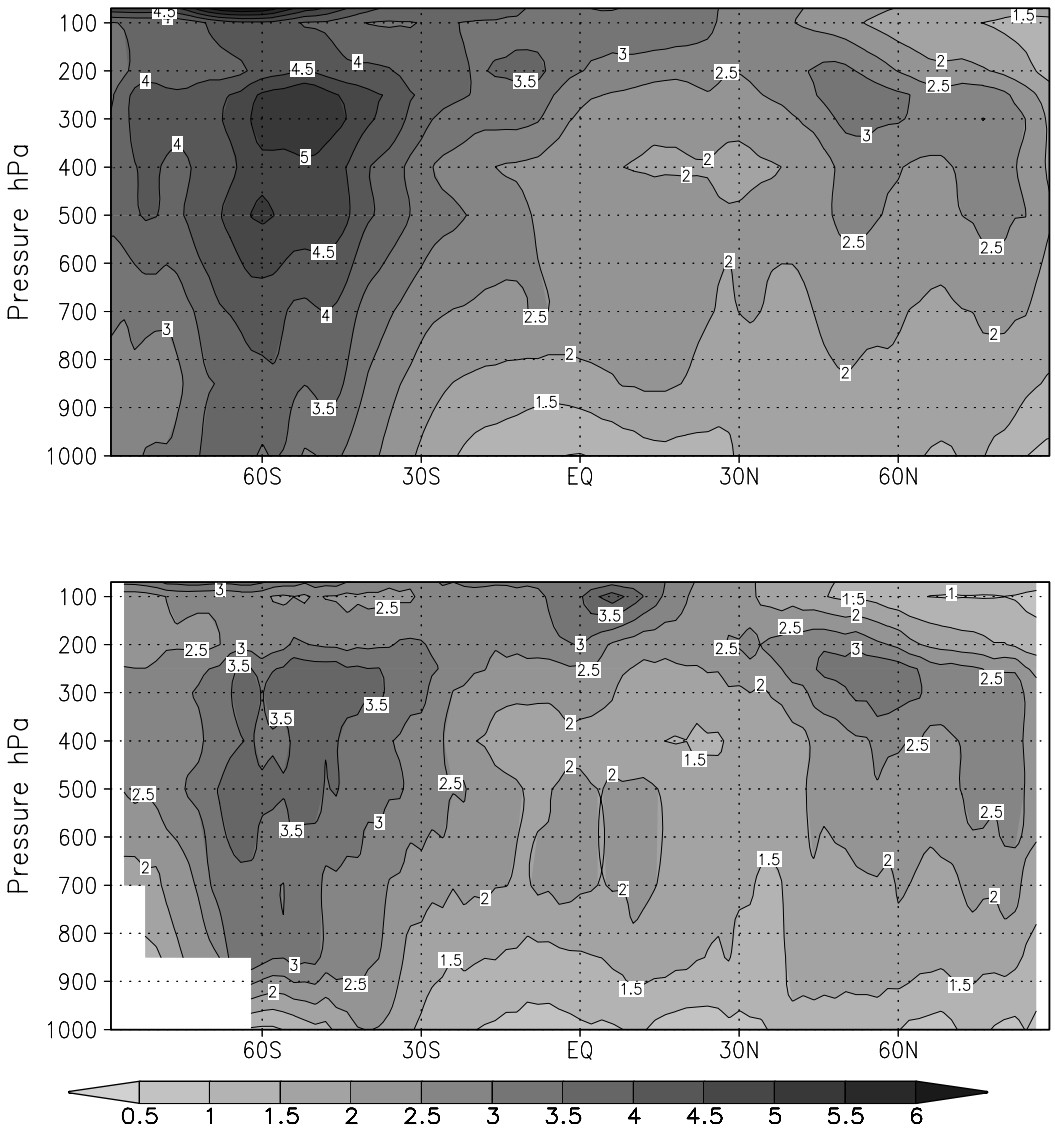

Fig. 4. Zonal mean standard deviation of total wind error: the output from the PSAS height-wind covariance model (top panel); calculated directly from the difference ensemble scaled by the global scaling constant (bottom panel).

$$\partial_{\mathrm{m}}(\cdot) \equiv \frac{\partial(\cdot)}{\partial\varphi} \,, \tag{3}$$

$$\partial_{\mathrm{l}}(\cdot) \equiv \frac{\partial(\cdot)}{\cos\varphi\partial\lambda} \,. \tag{4}$$

The height-wind forecast error covariance is modeled based on Equations (1) and (2), detailed in Guo et al. (1998).

2.2 *Computation in the NMC-method*

Figure 1 schematically depicts the components and procedures of the method employed in this study. The upper part outlines the computations in the NMC-method, starting the collection of a time series, or an ensemble, of lagged-forecast difference in height and wind fields between 24- and 48-hour forecasts valid at the same verification time. These differences are denoted by $\{\delta_{\mathrm{p}}\}$. The variances, i.e., the diagonals of the covariance matrix $\langle\delta_{\mathrm{p}}, \delta_{\mathrm{p}}^{\mathrm{T}}\rangle$, derived from the ensemble, are considered as the approximation of forecast error variances, where $\delta_{\mathrm{p}}^{\mathrm{T}}$ denotes the transpose of δ_{p}. The differences in the height and wind fields are treated as surrogates of the forecast errors. In the following description of the NMC-method, the term error is used in general, though it may refer to the differences.

The data used in the computation are the output of the 5-day height and wind component forecast laun-

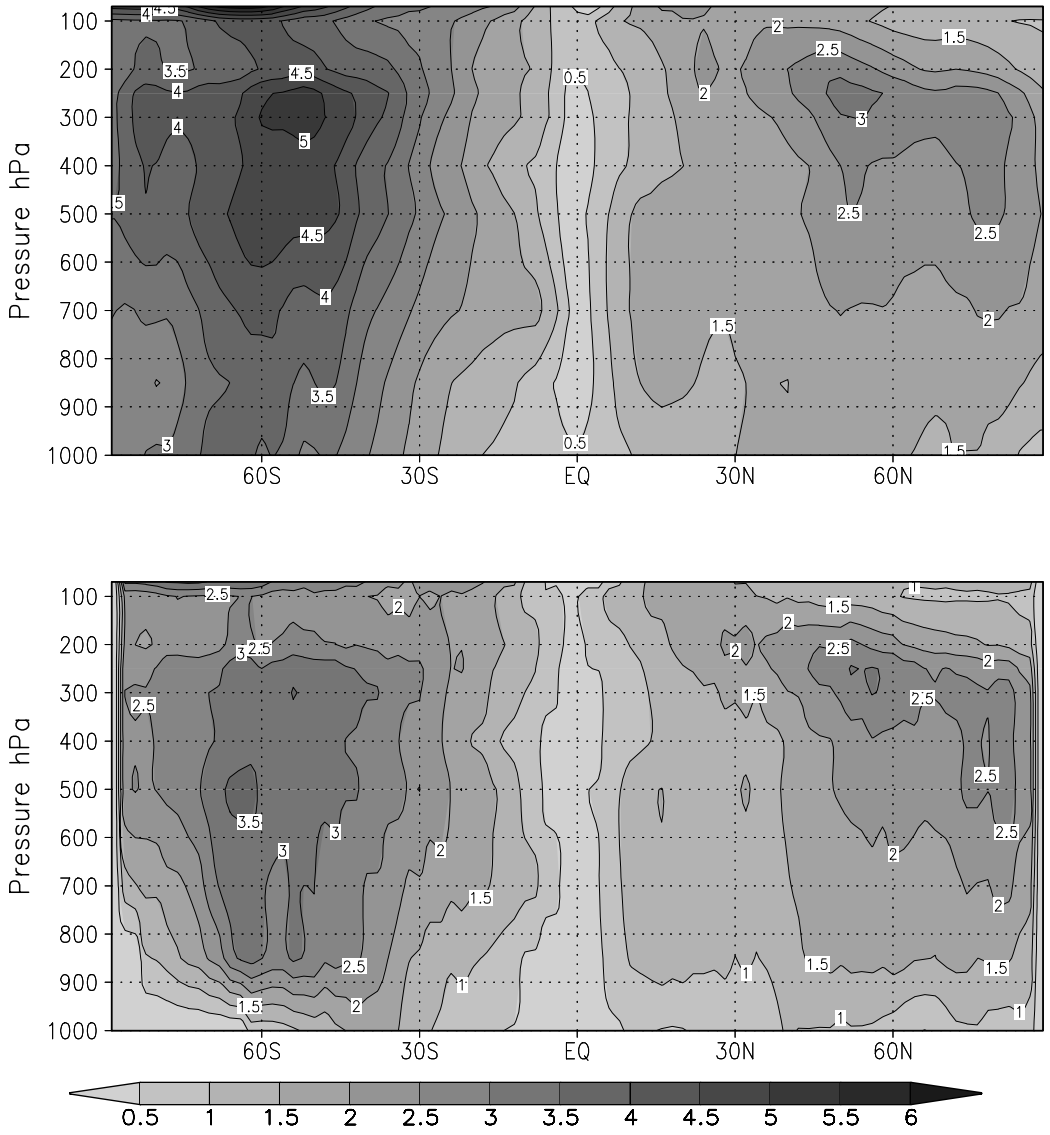

Fig. 5. Similar to Fig. 4, but for the zonal mean standard deviation of the coupled wind forecast error.

ched every day along with the assimilation of GMAO data assimilation system (DAS) (DAO, 1996) for the month of August 2002. Nineteen pressure levels are selected in the computation. The four coupling coefficients of Eq. (1) are derived, for each time record at each selected vertical pressure level, by least-square estimation with the one-month-long time series of the height and wind difference fields. The coupling coefficients are approximated as functions of latitude and are calculated within 4°-latitude bins. Note that the coupling coefficients are near zero over the Tropics; gradually increase with latitude; and reach high values in the mid latitudes. The monthly mean coupling coefficients are then calculated for each bin and substituted back into Eq. (1) to get the coupled wind error at each grid point for each time record. Subsequently, the decoupled wind errors are calculated as the residual of the coupled wind error from the total wind error. The stream function and velocity potential are derived from the decoupled wind error as described by Equations (2), (3), and (4) for each grid and each time record.

The final step is to calculate the error variances for height, streamfunction, and velocity potential: $\langle h^2 \rangle, \langle \psi^2 \rangle$, and $\langle \chi^2 \rangle$, respectively. Similarly, the error variances of the coupled and decoupled wind are computed. We use an angle bracket to denote the variances obtained by using the NMC-method and Greek letters to denote the variances obtained by using MLE, or truth, hereafter. In addition to the variances, the

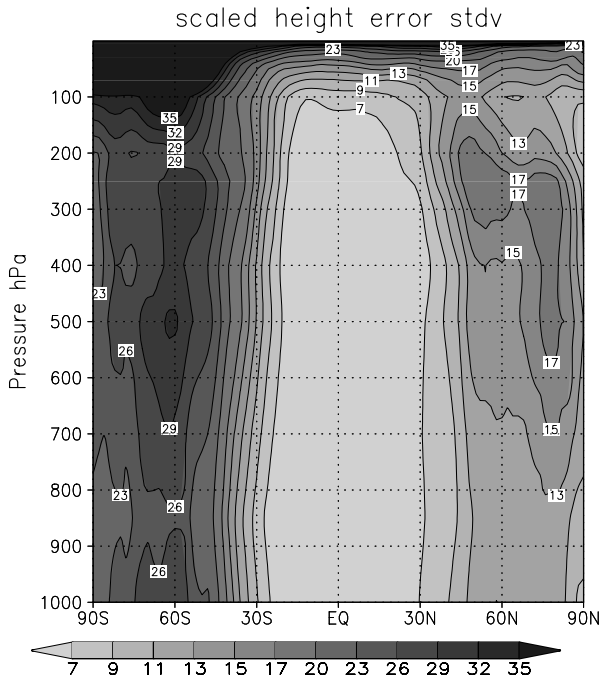

Fig. 6. Zonal mean standard deviation of forecast height error directly derived by using the NMC-method scaled by the scaling constant.

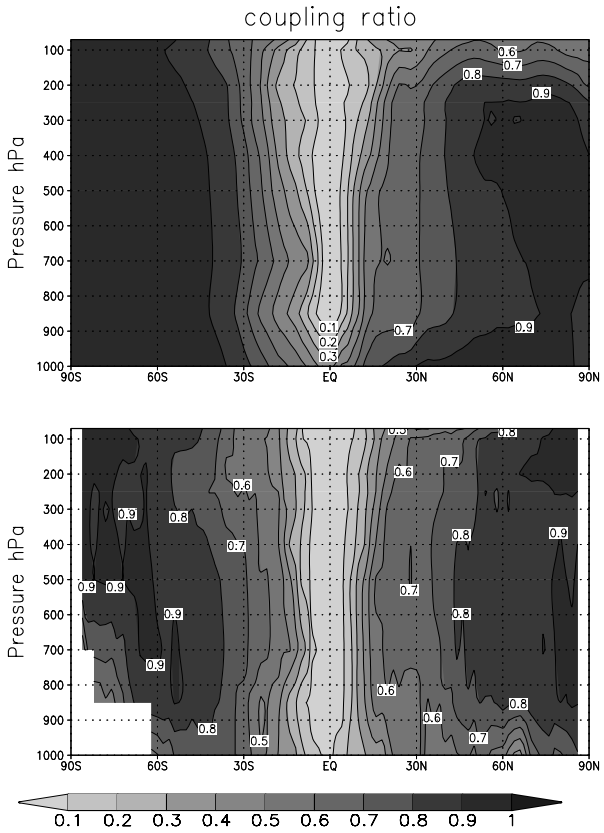

Fig. 7. Zonal mean coupling ratio, defined as the error variance ratio of the coupled wind to the total wind. Top: computed from the output of the PSAS covariance model, bottom: computed from the NMC-method.

globally averaged error horizontal correlation lengths, L_h, L_ψ, and L_χ, are derived for height, streamfunction, and velocity potential, respectively. The derivation is not straight-forward. It starts from the calculation of normalization factors of differentiated correlation functions evaluated on constant pressure levels. Once a normalization factor on a given pressure level is known, the horizontal length of a given correlation function model can be uniquely determined, either analytically or iteratively. Note that the NMC-method is able to provide the 2-dimensional normalization factors of the differentiated correlation function for the latitudinal direction and for the vertical levels. These values are averaged globally. All the computation formulas used here are documented in Guo (2005).

The vertical correlation lengths are also required by the error covariance model. However, in this study, we only consider the adjustment of horizontal correlation length and leave the vertical correlation lengths as they are in the previous operational system. This simplifies the tuning of the horizontal correlation length. The error variances along with the correlation lengths are the input of the height-wind forecast error covariance model of PSAS. Note that in the current version of the model, the variances are prescribed as functions of latitude and vertical level only. So zonal averaging is applied to these statistics to fit the form as prescribed in the covariance model.

2.3 *Maximum-likelihood estimation*

Dee and Da Silva (1999) derived the relationship between an error covariance model and the observed-minus-forecast residuals. They applied the maximum-likelihood method to the parameter estimation of observation and forecast error covariance models. As described in the paper, the actual sequence of the residuals v_k is considered as a realization of a multivariate stochastic process V_k, whose joint probability density function (pdf) is $p(v_k; \alpha)$. If the functional form of the pdf is known, then its value for a fixed dataset $v_k, k = 1, ..., K$ depends on α only: the function of α thus defined is called the likelihood function. The maximum-likelihood estimate $\hat{\alpha}$ is obtained by finding the maximum of the likelihood function. In their application, they postulate the stochastic process is white and Gaussian, and consider rawinsonde observation unbiased measurements of the true atmospheric state. The important issues are discussed and addressed along with the evidence of the advantage of the method in Dee and Da Silva (1999) and Dee et al. (1999). Recently, Dee extended the method to a height-wind forecast error covariance model to obtain height and wind error standard deviations, $\sigma_{h,\mathrm{ML}}$, and

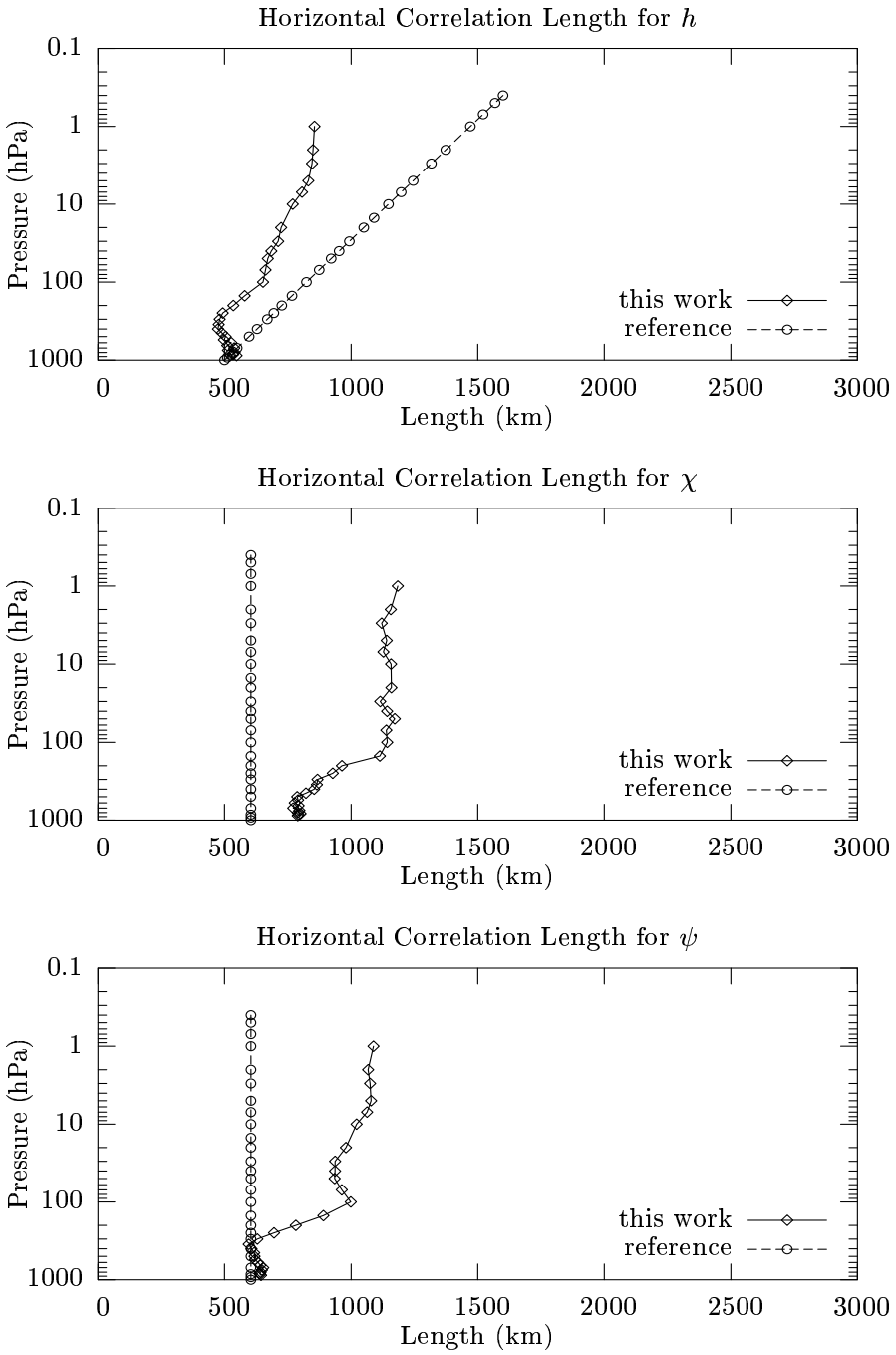

Fig. 8. Horizontal correlation length for height (top), velocity potential (middle), and streamfunction (bottom). Dashed line with open circle: values used in a previous system; solid line with diamonds: derived using the NMC-method within the framework of PSAS error covariance model.

$\sigma_{u,\mathrm{ML}}, \sigma_{v,\mathrm{ML}}$, (personal communication). This recent version of MLE is used in this study.

3. Calibration procedure

As shown in Fig. 1, maximum-likelihood estimation (Dee and Da Silva, 1999) is applied to radiosonde observed-minus-forecast residuals generated by the same version of GMAO DAS is used in the NMC-method. The forecast errors are estimated with the observations over six selected regions: the Eastern

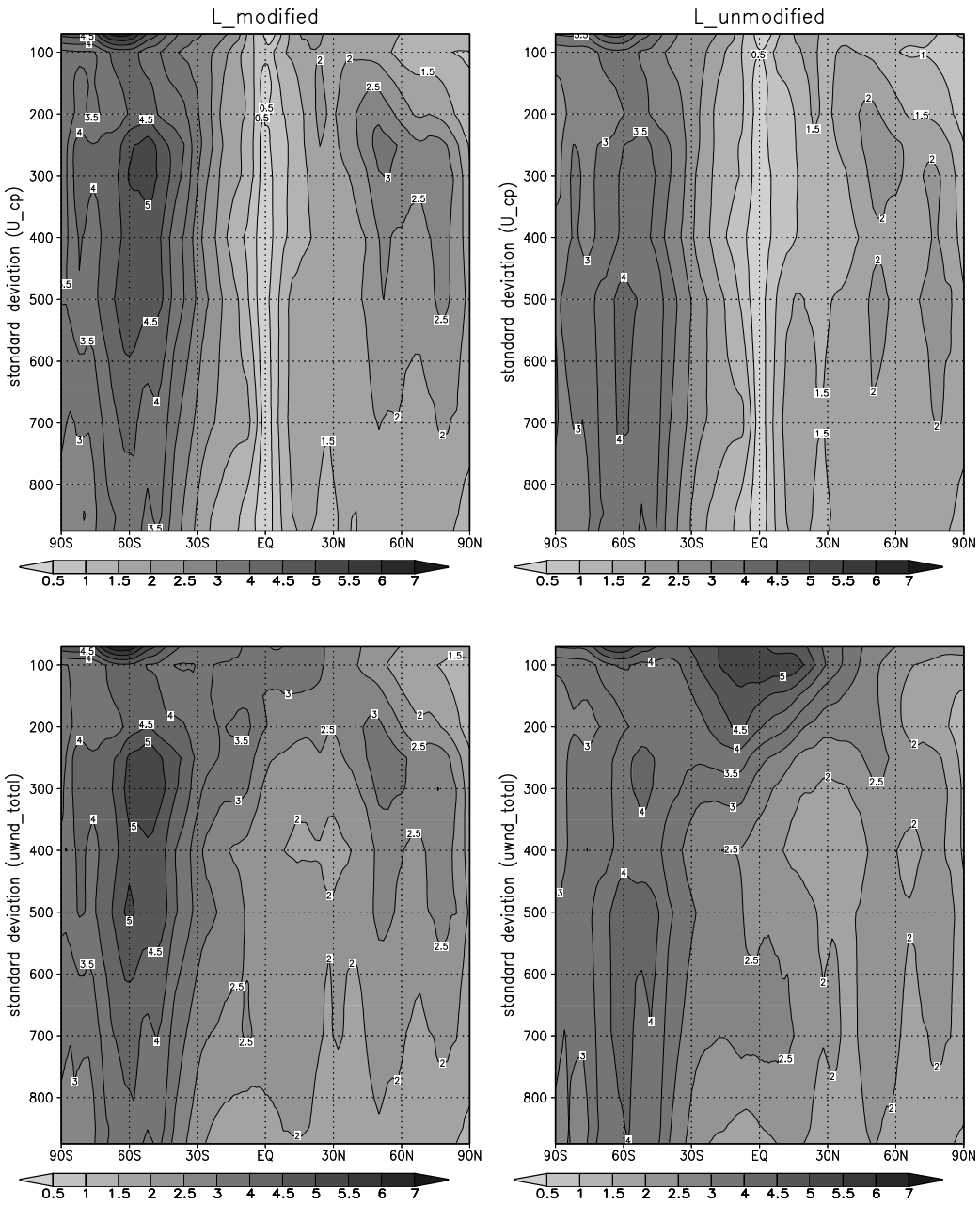

Fig. 9. Results of the experiment with the modified horizontal correlation length derived from the NMC-method (left column). Results of the experiment without the modification (right column). Top panels: standard deviation of coupled wind error; bottom panels: standard deviation of total wind error.

U.S., Arctic region Eastern Europe, Eastern China, Australia, and India. For the NMC-method the regional means of the error standard deviations are calculated using all the grid points in the same six regions and at the same vertical levels as in the MLE. Note that the NMC method in this case has a larger sample size than in the MLE. Figure 2 contrasts the standard deviation of height error $\sqrt{\langle h^2 \rangle}$ derived from the NMC-method (left panel) with that derived from MLE (right panel), exhibiting clear differences in the vertical profiles.

The NMC-method generates a clean pattern with a maximum around the upper tropospheric jet region and a minimum around 100 hPa uniformly over all six regions, whereas the results of the MLE do not resemble this pattern well (the Indian region is not plotted

here). It is hard to tell whether the values between the left and right panels are proportional. However, in Fig. 3, the ratios of $\sigma_{h,\mathrm{ML}}$ to $\sqrt{\langle h^2 \rangle}$ are quite consistent over the five regions. It is encouraging that the ratios are fairly consistent within the range of $0.5-1.0$ below 300 hPa over all regions, except India. Therefore, using a global scaling constant in the rescaling is feasible, except for the levels above 300 hPa where the ratios are divergent. We notice that the minimum at about 100 hPa is erroneously small compared with the previous findings, such as in Hollingsworth and Lönnberg (1986).

The calibration procedure requires a choice of calibration variable. We choose the standard deviation of forecast height error, $\sigma_{h,\mathrm{ML}}$, as the truth, since the height forecast errors are small in general, and the model errors occur predominantly at large scales. The calibration formula is then set up as shown in Fig. 1. The global scaling constant $\bar{\gamma}$ is obtained by averaging the γ of the five regions with an equal weight. The Indian region is treated as an outlier and not included (solid line in Fig. 3). This $\bar{\gamma}$ is multiplied by the zonal mean error standard deviation, SD, of the height, stream function, and velocity potential. These rescaled SDs, along with the four coupling coefficients and the correlation lengths, enter into the covariance model of PSAS to generate the forecast covariance matrix (rescaling process in Fig. 1). PSAS computes the components of the wind error statistics, including total wind $\sigma_{u,\mathrm{tot}}$, coupled wind $\sigma_{\mathrm{c},u}$, decoupled divergent wind $\sigma_{u,\text{d-div}}$, and decoupled rotational wind $\sigma_{u,\text{d-rot}}$. The v components are specified the same as the u.

4. Results

4.1 *Consistency of the method*

We first evaluate the consistency of the method by comparing the output of the PSAS covariance model with the SD directly derived from the forecast difference ensemble scaled by $\bar{\gamma}$. Figure 4 shows the zonal mean of the SD of the total forecast wind error generated from PSAS (top) and the one directly calculated from the ensemble of the difference scaled by $\bar{\gamma}$ (bottom). In general, the pattern and magnitudes are quite similar. This agreement indicates that the height-wind forecast error covariance model of PSAS is able to reproduce the forecast error statistics derived directly from the ensemble, even if several simplifications are taken in the implementation of the error covariance model.

However, over the middle latitudes of the Southern Hemisphere (SH), the magnitudes in the top panel are slightly larger than those in the bottom panel. We will see more discrepancies over the SH below.

Figure 5 shows the zonal mean coupled wind error SD from the output of the PSAS (top) and from the calculation using Eq. (1) with the coupling coefficients derived from the regression (bottom). Similarly, like in Fig. 4, the patterns and magnitude are comparable in the Northern Hemisphere. Over the SH, large differences exist in both shape and magnitude. Obviously, these differences contribute to the differences in the total wind error. The asymmetry of the wind forecast error in the two hemispheres is clearly due to that of the height error SD as shown by Fig. 6. It is clear that, by comparing Figs. 4 and 5 with Fig. 6, the large height error SD over the SH is responsible for the large coupled wind error, and therefore, the large total wind error.

Figure 7 shows the coupling ratio, which is defined as the error variance ratio of the coupling wind to the total wind. There is great similarity between the two panels over the NH. Over the SH, the results of the NMC-method (bottom) exhibit small structures, whereas the output of the covariance model is more smooth and uniform (top). One possible explanation for this discrepancy is the use of a global constant correlation length, which is one of the simplifications taken in the implementation of the forecast error covariance model in the PSAS. Previous studies have pointed out that the correlation lengths vary with latitude (e.g., Ingleby, 2001)

4.2 *Impact of horizontal correlation length*

The horizontal correlation function is an important component in a forecast covariance model. The differences in horizontal correlation lengths are significant between a previous system used for comparison in this study and the NMC-method, particularly above the levels of the middle troposphere. Fig. 8 shows the horizontal correlation length for height (top), velocity potential (middle), and streamfunction (bottom), where the dashed line with open circles denotes the values used in the previous system ("reference") and the solid line with diamonds denotes the values derived using the NMC-method ("this work"). In the previous system, a constant correlation length is used for both stream-function and velocity potential. Note that the curves from the NMC-method demonstrate clear transitions from the levels below 300 hPa to the levels above 100 hPa in all three cases.

In order to demonstrate the impact of the horizontal correlation length, one additional experiment is carried out with the same parameters as the previous experiment except using the unmodified horizontal correlation length. Figure 9 shows the result of this experiment (right column) and the comparison with the previous experiment (left column, same figures as the top panels in Figs. 4 and 5). The top panels are the standard deviation of the coupled wind error and the

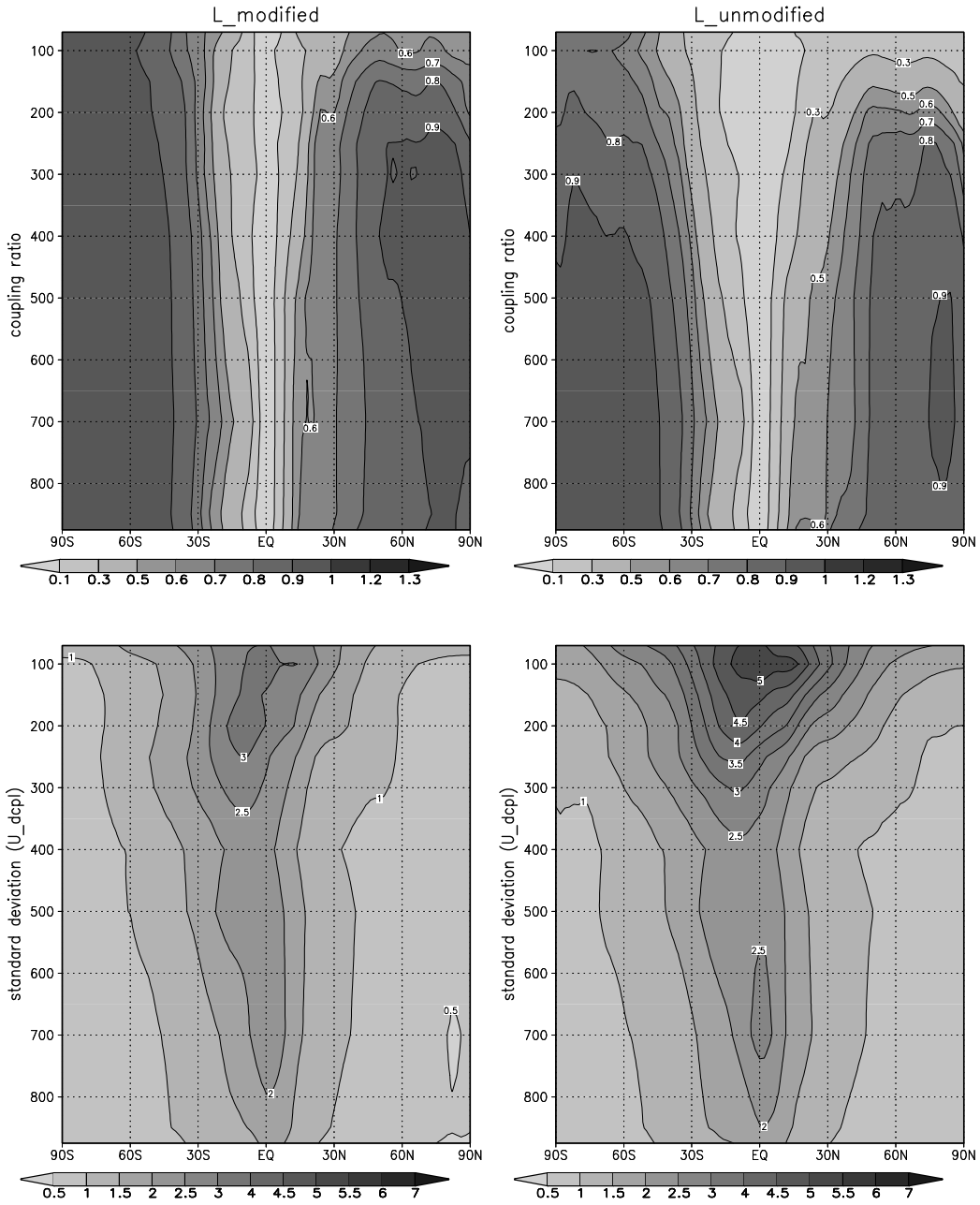

Fig. 10. Similar to Fig. 9 but for the coupling ratio (top panels) and the standard deviation of decoupled wind (bottom panels).

bottom are the standard deviation of total wind error. The impact of correlation length on the wind error components is obvious. In the experiment with unmodified correlation length, the patterns are significantly different, in particular, the misplacement of the tropospheric maximum center and the increased magnitudes around 100 hPa. Figure 10 shows a comparison of the coupling ratio (top panel) and the decoupled wind field (bottom). The experiment without the adjustment produces significant changes in both error pattern and values, departing from the fields obtained from the NMC-method. The coupling ratio is significantly reduced over the NH middle-high latitudes. This experiment indicates the importance of deriving and using parameters in a consistent way.

5. Summary and discussion

In this study, we apply an error statistics estimation method to the PSAS height-wind forecast error

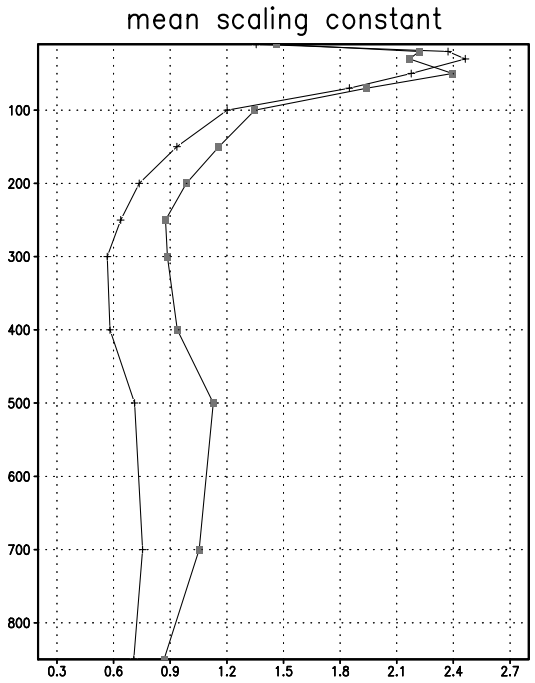

Fig. 11. Crosses: mean scaling value for the height error standard deviation averaged over the five regions. Squares: the ratio of the wind error standard deviation estimated by MLE to that derived from the NMC-method, averaged over the same five regions as used in MLE.

covariance model. The error statistics, estimated from one-month-long radiosonde height observed-minus-forecast residuals, are considered as the truth and used to rescale the error statistics obtained from the NMC-method. In general, a constant value for the globe is a good approximation for rescaling. The output of the PSAS error covariance model is examined and compared with the results of the NMC-method. The comparison exhibits great similarities indicating the consistency between the method and the error covariance model.The final product provides a full set of error statistics with a global pattern intrinsically constrained by the GCM model and with the magnitude of the 6-hour forecast error derived from the observation data.

This method provides a tool to tune a simple calibration variable $\bar{\gamma}$. Any available *a priori* information about forecast error may be incorporated into the calibration formula. With an appropriate calibration formula, all other parameters computed from the NMC-method are able to be rescaled in a consistent way.

Note that the height error SD here carries an austral winter (August) feature in the SH, a strong circulation within the jet region as shown in Fig. 6. For static forecast error statistics, the seasonal dependency should be removed by taking different season samples.

The height forecast error estimation from the NMC-method has a large uncertainty over the SH. In our MLE application, there is no information over this region. Although we expect the large error standard deviation there produced by the active dynamics and the large initial condition error due to less observation information, the magnitudes directly derived from the NMC-method are far too large relative to those over the NH.

Another uncertainty in the height error estimation appears just above the top of the tropopause as shown by Fig. 2 (left panel) in section 3. The results from the NMC-method underestimate the forecast error variance right above the tropopause compared with the findings of Lönnberg and Hollingsworth (1986) and others. One of the possible reasons is the large GCM error there. Further examination is needed to understand the problem.

The method can be further improved by using a second scaling constant in the calibration of the wind error statistics. The rational is that the model error, which is excluded in the NMC-method, is larger in the wind forecast than in the height forecast. The statistics of an ensemble of lagged-forecast difference mainly represents the error due to the initial condition difference, whereas the estimate from MLE includes both model error and initial error. Therefore the wind error derived by using the NMC-method is underestimated more than the height error estimation. Using the same one-month dataset, we computed the ratio of the wind error SD derived from MLE to that of the NMC-method in the same way as we did for height. In Fig. 11, the line with crosses is the $\bar{\gamma}$ for height, whereas the line with squares is that for wind calculated in the same way as that for height. It is clear that the ratio of the wind error statistics is larger than the $\bar{\gamma}$ of the height error statistics. A fine-calibration procedure could be applied with one additional scaling constant for the decoupled wind function.

This method inherits the limitations of the NMC-method, specifically, the limitations due to sparse observations and due to the timely small variation of a field. Moreover, the approach does not have the ability to include a flow-dependence in the forecast error statistics.

More recently, the traditional NMC-method has tended to be replaced by statistics on ensembles of forecasts. The ensemble method is more expensive than the lagged-forecast difference approach, though it might be easier to justify theoretically. This method is used at ECMWF and Meteo-France nowadays, and is believed to give better results (F. Bouttier, personal communication).

Acknowledgments. We thank Dr. Steve Bloom for his insightful discussion and encouragement throughout the course of this study. We are grateful to our colleagues Drs. Guang-Ping Luo and J. Jusem for providing

the computation programs and Dr. Fran Verter for providing the MLE computation. We thank Mr. Thomas Owens at GMAO for his help in processing the FVDAS data. A special thanks goes to our anonymous reviewers for their careful review and insightful comments.

REFERENCES

Dee, D., and A. M. da Silva, 1999a: Maximum-likelihood estimation of forecast and observation error covariance parameters. Part I: Methodology. *Mon. Wea. Rev.*, **127**, 1822–1834.

Dee, D., G. Gaspari, C. Redder, L. Rukhovets, and A. M. da Silva, 1999: Maximum-likelihood estimation of forecast and observation error covariance parameters. Part II: Applications. *Mon. Wea. Rev.*, **127**, 1835–1849.

DAO, 1996: Algorithm Theoretical Basis Document. Part D: Next Generation. [Available online at http://polar.gsfc.nasa.gov/sci_research/atbd.php.]

Guo, J., J. W. Larson, G. Gaspari, A. da Silva, and P. M. Lyster, 1998: Documentation of the physical-space statistical analysis system (PSAS). Part II: The factored-operator formulation of error covariances. DAO Office Note, 1998–04, 1–27.

Guo, J., 2005: NMC-method based computational forecast error covariance estimation and its implementation for the PSAS. Manuscript under preparation, available from GMAO, NASA/GSFC, MD 20771 USA.

Hollingsworth, A., 1989: The verification of objective analysis: Diagnostics of analysis system performance. *Meteorology and Atmospheric Physics*, **40**, 3–27.

Hollingsworth, A., and P. Lönnberg, 1986: The statistical structure of short-range forecast errors as determined from radiosonde data. Part I: The wind field. *Tellus*, **38A**, 111–136.

Ingleby, 2001: The statistical structure of forecast errors and its representation in the Met.Office Global 3-D Variational Data Assimilation Scheme. *Quart. J. Roy. Meteor. Soc.*, **127**, 209–231.

Lönnberg, P., and A. Hollingsworth, 1986: The statistical structure of short-range forecast errors as determined from radiosonde data. Part II: The covariance of height and wind errors. *Tellus*, **38A**, 137–161.

Parrish, D. F., and J. C. Derber, 1992: The National Meteorological Center's spectral statistical interpolation analysis system. *Mon. Wea. Rev.*, **120**, 1747–1763.